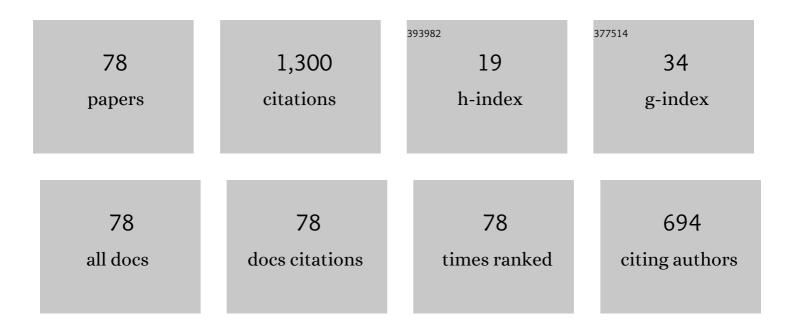


## List of Publications by Year in descending order

Source: https://exaly.com/author-pdf/7161802/publications.pdf Version: 2024-02-01



LINC CAO

#	Article	IF	CITATIONS
1	Rational design of a multifunctional molecular dye for dual-modal NIR-II/photoacoustic imaging and photothermal therapy. Chemical Science, 2019, 10, 8348-8353.	3.7	137
2	456-nm deep-blue laser generation by intracavity frequency doubling of Nd:GdVO4 under 879-nm diode pumping. Laser Physics, 2009, 19, 111-114.	0.6	106
3	Pulsed 456 nm deepâ€blue light generation by acoustooptical Qâ€switching and intracavity frequency doubling of Nd:GdVO <sub>4</sub> . Laser Physics Letters, 2008, 5, 577-581.	0.6	84
4	120-W continuous-wave diode-end-pumped Nd:GdVO_4 laser with high brightness operating at 912-nm. Optics Express, 2009, 17, 3574.	1.7	69
5	Room temperature efficient continuous wave and Q-switched Ho:YAG laser double-pass pumped by a diode-pumped Tm:YLF laser. Laser Physics Letters, 2008, 5, 800-803.	0.6	56
6	Diode-end-pumped acousto-optically Q-switched 914 nm laser and the pulsed blue light generation by intracavity frequency doubling. Laser Physics Letters, 2008, 5, 433-436.	0.6	54
7	Switchable Nanochannel Biosensor for H <sub>2</sub> S Detection Based on an Azide Reduction Reaction Controlled BSA Aggregation. Analytical Chemistry, 2019, 91, 6149-6154.	3.2	45
8	Long distance, distributed gas sensing based on micro-nano fiber evanescent wave quartz-enhanced photoacoustic spectroscopy. Applied Physics Letters, 2017, 111, .	1.5	44
9	Laser operation of LD end-pumped grown-together Nd:YVO <sub>4</sub> /YVO <sub>4</sub> composite crystal. Laser Physics Letters, 2008, 5, 429-432.	0.6	39
10	Discrimination of Human and Nonhuman Blood by Raman Spectroscopy and Partial Least Squares Discriminant Analysis. Analytical Letters, 2017, 50, 379-388.	1.0	34
11	Quasi-three-level Nd:GdVO <sub>4</sub> laser under diode pumping directly into the emitting level. Laser Physics Letters, 2008, 5, 797-799.	0.6	33
12	Diode-laser-pumped high efficiency continuous-wave operation at 912 nm laser in Nd:GdVO4crystal. Laser Physics Letters, 2009, 6, 34-37.	0.6	32
13	Efficient generation of 914 nm laser with high beam quality in Nd:YVO4crystal pumped byπ-polarized 808 nm diode-laser. Laser Physics Letters, 2008, 5, 655-658.	0.6	29
14	Upconversion spectra of Nd:GdVO <sub>4</sub> crystal under CW 808 nm diode-laser pumping. Laser Physics Letters, 2009, 6, 125-128.	0.6	28
15	All-solid-state continuous-wave yellow laser at 561Ânm under in-band pumping. Journal of the Optical Society of America B: Optical Physics, 2013, 30, 95.	0.9	26
16	8.9-W continuous-wave, diode-end-pumped all-solid-state Nd:YVO4 laser operating at 914 nm. Laser Physics, 2009, 19, 389-391.	0.6	25
17	Blood species identification based on deep learning analysis of Raman spectra. Biomedical Optics Express, 2019, 10, 6129.	1.5	24
18	Improved performance of acoustooptically Q-switched Nd:GdVO4 laser by using the planoconvex cavity. Laser Physics, 2008, 18, 1505-1507.	0.6	22

#	Article	IF	CITATIONS
19	Quasi-three-level Nd:YVO4 laser operation at 914 nm under 879 nm diode laser pumping. Laser Physics, 2010, 20, 1590-1593.	0.6	22
20	Active Q-switching operation of slab Ho:SYSO laser wing-pumped by fiber coupled laser diodes. Optics Express, 2019, 27, 11455.	1.7	20
21	Vitamin D levels correlate with lymphocyte subsets in elderly patients with age-related diseases. Scientific Reports, 2018, 8, 7708.	1.6	19
22	Comparison on performance of acousto-optically Q-switched Nd:GdVO_4 and Nd:YVO_4 lasers at high repetition rates under direct diode pumping of the emitting level. Optics Express, 2009, 17, 9468.	1.7	18
23	Continuous-wave and passively Q-switched 1.06μm ceramic Nd:YAG laser. Optics and Laser Technology, 2016, 81, 46-49.	2.2	17
24	Continuous-wave yellow–green laser at 056  μm based on frequency doubling of a diode-end-pumpe ceramic Nd:YAG laser. Applied Optics, 2015, 54, 5817.	d <sub>2.1</sub>	16
25	The application of bioactive pyrazolopyrimidine unit for the construction of fluorescent biomarkers. Dyes and Pigments, 2020, 173, 107878.	2.0	16
26	Laser operation at high repetition rate of 100ÂkHz in Nd:GdVO4 under 879Ânm diode-laser pumping. Applied Physics B: Lasers and Optics, 2008, 92, 199-202.	1.1	15
27	Diode-pumped short pulse passively Q-switched 912 nm Nd:GdVO4/Cr:YAG laser at high repetition rate operation. Laser Physics, 2010, 20, 1275-1278.	0.6	15
28	Discrimination of blood species using Raman spectroscopy combined with a recurrent neural network. OSA Continuum, 2021, 4, 672.	1.8	15
29	Fluorescent hydrogen sulfide probes based on azonia-cyanine dyes and their imaging applications in organelles. Analytica Chimica Acta, 2019, 1068, 60-69.	2.6	14
30	Error analysis of the spectral shift for partial least squares models in Raman spectroscopy. Optics Express, 2018, 26, 8016.	1.7	13
31	Dual-model analysis for improving the discrimination performance of human and nonhuman blood based on Raman spectroscopy. Biomedical Optics Express, 2018, 9, 3512.	1.5	13
32	Efficient continuous-wave 1112 nm Nd:YAG laser operation under direct diode pumping at 885 nm. Laser Physics Letters, 2013, 10, 015802.	0.6	12
33	Continuous-wave and passively Q-switched Nd:GYTO <sub>4</sub> laser. Laser Physics Letters, 2017, 14, 095802.	0.6	12
34	Continuous-wave yellow laser generation at 578 nm by intracavity sum-frequency mixing of thin disk Yb:YAG laser and Nd:YAG laser. Optics and Laser Technology, 2017, 92, 32-35.	2.2	11
35	Continuous-wave and pulsed 1,066-nm Nd:Gd <sub>069</sub> Y <sub>03</sub> TaO <sub>4</sub> laser directly pumped by a 879-nm laser diode. Optics Express, 2018, 26, 15705.	1.7	11
36	Improvement in the laser performances of an A-O Q-switched Nd:GdVO4 laser by direct-diode pumping into the emitting level. Laser Physics, 2008, 18, 831-834.	0.6	10

#	Article	IF	CITATIONS
37	Highly efficient continuous-wave composite Nd:YAG laser at 1,112Ânm under diode pumping directly into the emitting level. Applied Physics B: Lasers and Optics, 2013, 111, 407-413.	1.1	10
38	High-power continuous-wave yellow–green laser at 558nm under in-band pumping. Optics Communications, 2014, 319, 110-112.	1.0	10
39	Discrimination of human and nonhuman blood using Raman spectroscopy with self-reference algorithm. Journal of Biomedical Optics, 2017, 22, 1.	1.4	10
40	Improvement of diode-end-pumped 912 nm Nd:GdVO4 laser performance based on microchannel heat sink. Journal of Russian Laser Research, 2009, 30, 327-337.	0.3	9
41	Fourier based partial least squares algorithm: new insight into influence of spectral shift in "frequency domain― Optics Express, 2019, 27, 2926.	1.7	9
42	The influence of energy transfer upconversion on thermal loading in end-pumped Nd:GdVO4 laser. Laser Physics, 2009, 19, 1969-1973.	0.6	8
43	Effects of energy-transfer up-conversion and excited-state absorption in quasi-three-level Nd:GdVO4 lasers. Journal of Russian Laser Research, 2009, 30, 376-383.	0.3	7
44	<scp>Highâ€power</scp> , continuousâ€wave optical parametric oscillator based on <scp>MgO</scp> : <scp>sPPLT</scp> crystal. Microwave and Optical Technology Letters, 2021, 63, 2068-2073.	0.9	7
45	High Power Continuous-Wave and Acousto-Optic Q-Switched Nd:GdVO 4 Laser Operated at 912 nm. Chinese Physics Letters, 2008, 25, 119-121.	1.3	6
46	Investigation on 13 μm laser performance with Nd:Gd069Y03TaO4 and Nd:Gd068Y03NbO4 mixed crystals. Optics Express, 2018, 26, 15785.	1.7	6
47	High-repetition-rate passively Q-switched Nd:GdTaO4 1066â€⁻nm laser under 879â€⁻nm pumping. Infrared Physics and Technology, 2019, 102, 103025.	1.3	6
48	926â€ <sup>–</sup> nm laser operation in Nd:GdNbO4 crystal based on 4F3/2â€ <sup>–</sup> →â€ <sup>–</sup> 4I9/2 transition. Optics and Laser Technology, 2018, 101, 515-519.	2.2	5
49	Harmonic mode locking underneath the Q-switched envelope in passively Q-switched mode-locked Nd:GdTaO4 1066Ânm laser. Infrared Physics and Technology, 2020, 111, 103553.	1.3	5
50	The identification of blood species using the correlation coefficient of sub-spectra based on Raman spectroscopy. Optik, 2020, 200, 163312.	1.4	4
51	4F3/2→4I9/2 and 4F3/2→4I13/2 laser operations with a Nd:GdTaO4 crystal. Optics and Laser Technology, 2020, 131, 106444.	2.2	4
52	Study of the thermal effect in Nd:GdVO4 912 nm CW laser. Journal of Russian Laser Research, 2013, 34, 114-119.	0.3	3
53	Generation of a 578-nm Yellow Laser by the Use of Sum-Frequency Mixing in a Branched Cavity. IEEE Photonics Journal, 2016, 8, 1-7.	1.0	3
54	LD pumped passively Q-switched ceramic Nd:YAG 946Ânm laser with a high peak power output. Optical and Quantum Electronics, 2016, 48, 1.	1.5	3

#	Article	IF	CITATIONS
55	LD pumped 1347â€ <sup>-</sup> nm laser with a novel Nd:GdNbO4 crystal. Infrared Physics and Technology, 2018, 94, 32-37.	1.3	3
56	Synthesis and optical properties of bispyrazolopyridine derivatives. Dyes and Pigments, 2020, 181, 108569.	2.0	3
57	High Dynamic Range Structured Illumination Microscope Based on Multiple Exposures. Frontiers in Physics, 2021, 9, .	1.0	3
58	Determination of blood species using echelle Raman spectrometer and surface enhanced Raman spectroscopy. Spectrochimica Acta - Part A: Molecular and Biomolecular Spectroscopy, 2022, 281, 121640.	2.0	3
59	Quasi-three-level neodymium vanadate laser operation under polarized diode pumping: theoretical and experimental investigation. Laser Physics, 2012, 22, 1279-1285.	0.6	2
60	Research on the optical system of neonatal jaundice phototherapy apparatus based on fly-eye lens. , 2013, , .		2
61	Modeling and optimization of actively Q-switched Nd-doped quasi-three-level laser. Optics Communications, 2013, 305, 276-281.	1.0	2
62	Spectral Range Optimization to Enhance the Effectiveness of Phototherapy for Neonatal Hyperbilirubinemia. Journal of Applied Spectroscopy, 2017, 84, 92-102.	0.3	2
63	Comparison on performances of continuous-wave and acousto-optically Q-switched Nd:GdYTaO4 lasers under 808Anm and 879Anm pumping. Infrared Physics and Technology, 2020, 110, 103449.	1.3	2
64	High-efficiency Nd:LuVO <sub>4</sub> quasi-three-level 916Ânm laser under polarized pumping. Applied Optics, 2013, 52, 4020.	0.9	1
65	High-power, high-repetition-rate actively Q-switched 916nm laser and the frequency doubled pulsed 458nm blue laser. Optics and Laser Technology, 2014, 58, 161-165.	2.2	1
66	Diode-pumped passively Q-switched 916nm laser with a Cr4+:YAG saturable absorber. Optics Communications, 2014, 313, 401-405.	1.0	1
67	Modeling and optimization of actively Q-switched Nd:GdVO4 912 nm laser. Optik, 2015, 126, 1282-1286.	1.4	1
68	Diode pumped Dy:YAG yellow laser. , 2017, , .		1
69	Novel CW and actively Q-switched 1066 nm Nd:GdYNbO4 laser under direct pumping. Optik, 2019, 181, 398-403.	1.4	1
70	The singleâ€wavelength 561 nm laser based on reflective volume Bragg grating. Microwave and Optical Technology Letters, 2023, 65, 1255-1260.	0.9	1
71	Improvement of the Performance of an Acousto-Optical Q-Switched Nd:YAG 946Ânm Laser Using a Convex–Plane Cavity. Journal of Russian Laser Research, 2013, 34, 586-592.	0.3	0
72	All-Solid-State Efficient CW Yellow Laser under Direct Diode-Pumping. , 2014, , .		0

#	Article	IF	CITATIONS
73	Quasi-three-level Nd:GdYNbO <sub>4</sub> 927 nm laser under 879 nm laser diode pumping. Laser Physics, 2018, 28, 085803.	0.6	Ο
74	LD pumped quasi-three-level 928â€⁻nm laser with Nd:Gd0.69Y0.3TaO4 mixed crystal. Optics and Laser Technology, 2019, 111, 222-226.	2.2	0
75	All-Solid-State Continuous-wave Yellow-Green Ceramic Laser at 0.56 μm. , 2015, , .		Ο
76	LD pumped Nd:GdNbO4 crystal laser operating at 926 nm. , 2018, , .		0
77	Tunable short-wave near-infrared continuous wave source based on a 532â€nm pumped singly resonant optical parametric idler oscillator. , 2022, 1, 547.		Ο
78	High peak power, high repetition rate electro-optically Q-switched Nd:GdTaO4 1066Ânm laser. Infrared Physics and Technology, 2022, 125, 104266.	1.3	0